

Growth of GaAs Epitaxial Microcrystals on an S-Terminated GaAs Substrate by Successive Irradiation of Ga and As Molecular Beams

Nobuyuki KOGUCHI and Keiko ISHIGE

National Research Institute for Metals, Tsukuba Laboratories, 1-2-1 Sengen, Tsukuba, Ibaraki 305

(Received July 28, 1992; accepted for publication March 13, 1993)

Numerous GaAs epitaxial microcrystals with an average base size of $250 \text{ \AA} \times 430 \text{ \AA}$ with (111) facets were fabricated on a sulfur-terminated (S-terminated) GaAs (001) substrate with successive irradiation of Ga and As molecular beams. The growth of GaAs microcrystals on the S-terminated substrate was caused by a vapor-liquid-solid (VLS) mechanism. This phenomenon originated in the inertness for the adhesion of Ga and As molecules and nearly equal lattice constants of the S-terminated GaAs surface and GaAs surface. This method, called droplet epitaxy, is thought to show promise as a growth method for fabricating GaAs quantum well boxes.

KEYWORDS: MBE, MEE, S-termination, VLS, quantum well boxes

1. Introduction

Predictions of enhanced electron mobility device¹⁾ and advanced semiconductor laser with high-monochromized and low threshold current density²⁾ have been made for the applications of quantum well box systems. Recently, selective metalorganic vapor phase epitaxy for fabricating quantum well boxes was demonstrated.³⁾ Molecular beam epitaxy (MBE) is successfully used in the growth of finely layered structures and quantum well wires. However, comparable success has not been achieved in the production of structures for quantum well boxes.

We have proposed a new MBE growth method called droplet epitaxy for the fabrication of some III–V compound semiconductor epitaxial microcrystals on a II–VI compound semiconductor substrate for quantum well boxes.^{4–6)} This method is based on V-column element incorporation into the III-column element droplets deposited on the inert substrate for the monolayer adsorption of the III- and V-column elements. It is also necessary for the substrate to have a lattice constant nearly equal to that of the microcrystals with a zincblende structure for the epitaxial growth of the microcrystals.

Some III–V compound surfaces terminated with a VI-column element such as S, Se or Te have been reported as providing an inert surface for foreign atom adhesion caused by the almost filled dangling bonds on the surface.^{7–10)} The III–V compound semiconductor surface terminated with the VI-column element is thought to be suitable for the growth of epitaxial microcrystals by droplet epitaxy. In this paper, we describe three-dimensional growth of GaAs epitaxial microcrystals on a sulfur-terminated (S-terminated) GaAs substrate by droplet epitaxy.

2. Experimental

The MBE system used in this work was a conventional system (ANELVA-620) with a sample introduction chamber, a cluster of 40 cm^3 boron nitride effusion cells in a common liquid nitrogen shroud and an electron gun for reflection high-energy electron diffraction (RHEED) with a primary beam energy of 30 keV. The system was capable of obtaining an ultimate pressure

in the 10^{-10} Torr range. Elemental Ga and As in the Knudsen cells were used as molecular beam sources.

First, the GaAs (001) surface was cleaned using $\text{H}_2\text{SO}_4:\text{H}_2\text{O}_2:\text{H}_2\text{O}=6:1:1$ for 3 min at 70°C , and heated in the As molecular beam flux with a beam equivalent pressure of 6×10^{-6} Torr at 590°C for 30 min to obtain a well-defined (2×4) As-stabilized surface. After the substrate temperature was decreased to room temperature, the sample was removed from the MBE chamber and immersed in the $(\text{NH}_4)_2\text{S}_x$ solution within 10 s for 30 min at room temperature and then heated in the MBE chamber again at 400°C for 30 min without an As molecular beam to obtain an S-terminated surface using the same procedure as that of Oigawa *et al.*⁹⁾ During this procedure, the As cell was kept at room temperature.

Next, the Ga droplets were deposited on this substrate surface at 200°C for 20 s. The total amount of Ga was equivalent to 2.7 monolayers of GaAs. After the deposition of the Ga droplets, the As cell was heated to obtain an As_4 molecular beam with equivalent pressure of 3×10^{-6} Torr and the As cell shutter was opened. Arsenic molecular beam flux estimated from the beam equivalent pressure was $5.8 \times 10^{14} \text{ cm}^{-2} \text{ s}^{-1}$. Beam intensity of Ga from the effusion cell was determined from the periods of the RHEED specular beam intensity oscillation during MBE growth of GaAs, while the As_4 beam intensity was obtained from the beam equivalent pressure measured by a flux monitor gauge placed at the same position as the substrate, using the equations given in refs. 11 and 12 in the same manner as Horikoshi *et al.*¹³⁾

For comparison, the same procedure was performed for the As-adsorbed GaAs (001) substrate with a surface structure of $c(4 \times 4)$ at 200°C . The surface was obtained by decreasing the substrate temperature and the As cell temperature after obtaining a (2×4) surface structure in the As molecular beam flux at 590°C for 30 min.

The structures of the surfaces of the samples were observed using a field-emission-type high-resolution scanning electron microscope (HRSEM).

3. Results and Discussion

3.1 Change in the RHEED patterns

The RHEED patterns observed at each stage of the growth process on the S-terminated GaAs substrate along complementary $\langle 110 \rangle$ and $\langle 1\bar{1}0 \rangle$ azimuths are shown in Fig. 1. The surface reconstruction of the sample before removal from the MBE chamber after annealing in the As molecular beam flux was $c(4 \times 4)$, which corresponded to the As-adsorption phase.¹⁴⁾ The surface reconstruction was (1×1) at room temperature after immersion in $(\text{NH}_4)_2\text{S}_x$, which changed to (2×1) with heating above about 250°C similar to other researchers' results for S-termination⁷⁻⁹⁾ and cooling to 200°C for the deposition of Ga. Diffraction patterns such as halos and (2×1) reconstruction were observed simultaneously on the Ga-deposited surface. The halo is caused by the diffraction of Ga droplets deposited on the substrate surface. After the As molecular beam irradiation, the RHEED pattern changed to one with spotty features with streaks along the $\langle 111 \rangle$ azimuth. The $\langle 111 \rangle$ streaks were clearly observed along the $\langle 110 \rangle$ azimuth rather than along the $\langle 1\bar{1}0 \rangle$ azimuth. Some twin spots were observed along both azimuths.

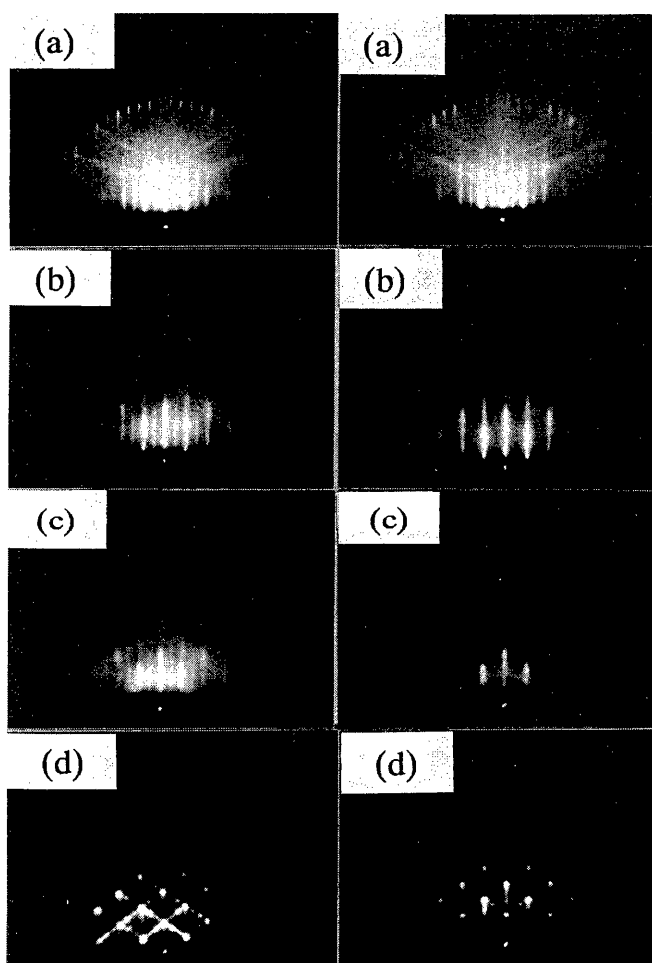


Fig. 1. The RHEED patterns observed at each stage of the growth process on the S-terminated GaAs substrate. (a) is the pattern immediately before removal from the MBE chamber. (b) is the pattern after the S-termination with annealing of the sample at 400°C. (c) is the pattern after the Ga deposition at 200°C. (d) is the pattern after the As molecular beam irradiation at 200°C. Left column: electron beam along $[110]$; right column: electron beam along $[1\bar{1}0]$.

The (2×1) surface reconstruction disappeared with the appearance of transmission spots. This is caused presumably by the difference in the transparency of the electron beam through the droplets and the microcrystals, because the portion of the substrate surface between Ga droplets or microcrystals remains an original S-terminated surface. Indeed, the (2×1) surface reconstruction did not change with the As molecular beam irradiation without the deposition of the Ga droplets.

In contrast, the halo and (1×1) surface structure appeared after the Ga deposition on the As-adsorbed GaAs (100) substrate with the surface structure of $c(4 \times 4)$ at 200°C. Figure 2 shows the change in the RHEED patterns during the same procedure on the $c(4 \times 4)$ As-adsorbed GaAs surface. The halo disappeared and (1×3) streaks with nodes appeared after the As molecular beam irradiation to this sample surface. The (1×3) surface structure is known as an As-adsorption phase at low temperatures.¹⁴⁾

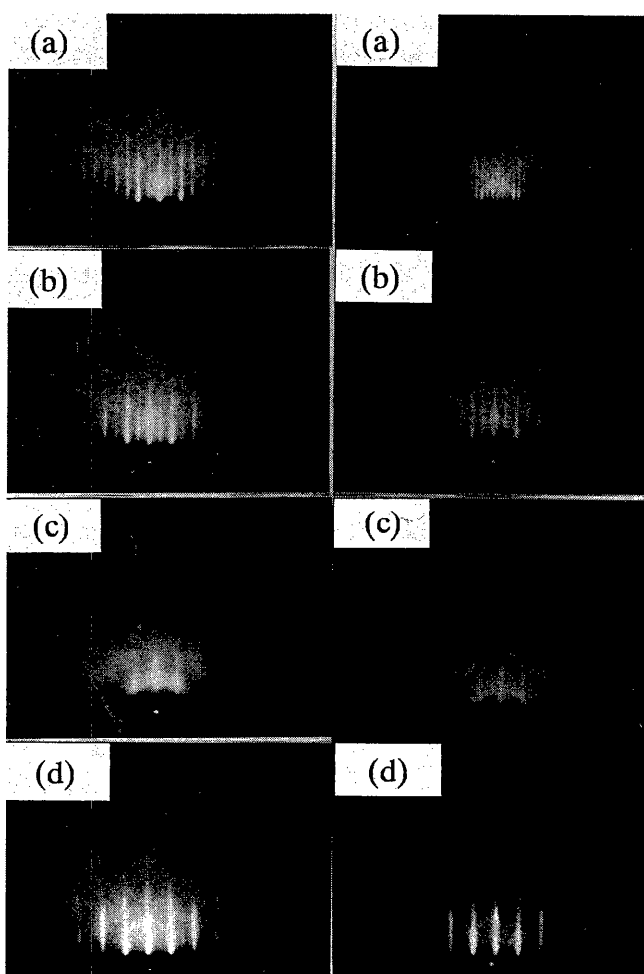


Fig. 2. The RHEED patterns observed at each stage of the growth process on the As-adsorbed GaAs substrate. (a) is the pattern after annealing of GaAs at 590°C in the As molecular beam. (b) is the pattern after decreasing the substrate temperature to 200°C. (c) is the pattern after the Ga deposition at 200°C. (d) is the pattern after the As molecular beam irradiation at 200°C. Left column: electron beam along $[110]$; right column: electron beam along $[1\bar{1}0]$.

3.2 Variations in RHEED intensities

The changes in the specular beam, halo and (004) transmission diffraction intensities are shown in Fig. 3 for the same procedure on the surface of S-terminated GaAs. The halo intensities were measured at the most intensive point of the radial distribution of the diffraction. The specular beam intensity was observed along the $[110]$ azimuth at an incident angle of 1.5° .

The intensity of the specular beam decreased monotonously with the Ga deposition and showed no change with the As molecular beam irradiation. The halo intensity increased immediately after the Ga deposition and decreased with the As molecular beam irradiation. The halo intensity shows a maximum and decreases slightly during Ga deposition. This phenomenon is caused by the absorption of the electron beam by the droplets, because the size of the Ga droplets increased with increasing deposition time. The intensity of the (004) transmission diffraction spot increases gradually as the halo disappears with the As molecular beam irradiation. The halo disappeared after about 20 s irradiation of As molecular beam to the droplets with beam equivalent pressure of 3×10^{-6} Torr. Since the average diameter of a Ga droplet is 240 Å as mentioned below, the total number of As atoms impinging directly on a single droplet for 20 s is estimated as 2×10^5 atoms, which is nearly equal to the number of Ga atoms in the droplet. This coincidence suggests that the GaAs microcrystals grow by the direct incorporation of As atoms from the molecular beam.

These changes in the RHEED intensities showed that the impinging Ga atoms coalesced and formed droplets without reacting with the surface first and then the three-dimensional growth of GaAs epitaxial microcrystals occurred by the subsequent As molecular beam irradiation. Ohno and Shiraishi⁸⁾ revealed that

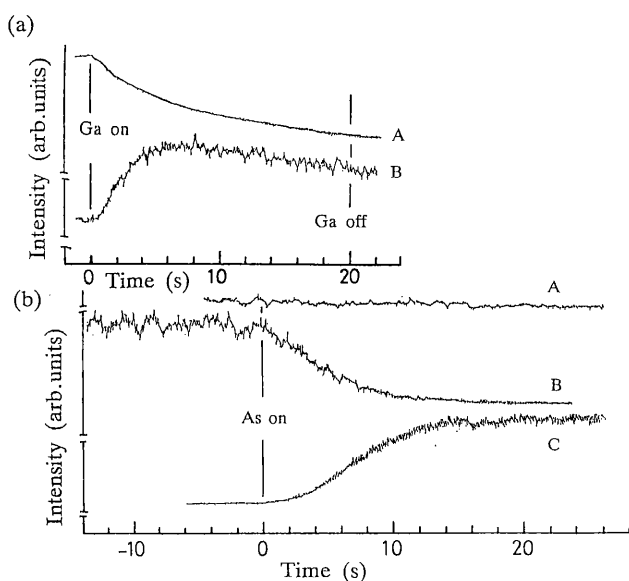


Fig. 3. The variations in the RHEED intensities during Ga deposition (a) and the As molecular beam irradiation (b) on the S-terminated GaAs substrate at 200°C . A, B and C correspond to the specular beam, halo and (004) transmission spot intensities, respectively.

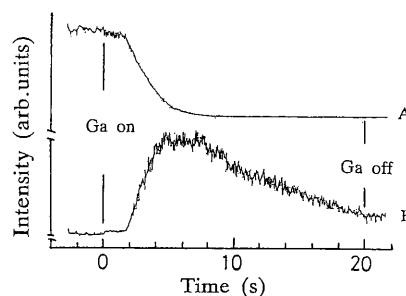


Fig. 4. The variations in the specular beam A and halo B intensities during Ga deposition on the S-terminated GaAs substrate at 350°C .

the monolayer of S combined with the outermost Ga atoms of the substrate surface, and the S atoms occupied the bridge site on the surface. The presence of almost filled dangling bonds on the S-terminated surface prevents the adsorption of foreign atoms. Although the compounds of Ga and S, i.e., GaS and Ga_2S_3 , have greater heat of formation than GaAs¹⁵⁾ and are thus thought to be more stable than GaAs, these compounds were not formed on the substrate surface during Ga deposition at the substrate temperature of 200°C . This is presumably due to the activation energy required for the reaction between Ga and S. In fact, the (2×1) pattern was weaker and more diffused when Ga was deposited at a higher temperature, *e.g.*, 350°C . Figure 4 shows that the RHEED intensities change during Ga deposition on the S-terminated GaAs surface at 350°C . The intensities of the specular beam and halo change rapidly after the incubation time of about 2 s. Since the Ga deposition rate is the same as in the case of the substrate temperature of 200°C , the incubation time suggests that some reaction occurred between Ga and S at 350°C . From the incubation time, the amount of Ga participating in the reaction with S atoms is estimated to be about 0.25 monolayers at this temperature.

Wagner and Ellis¹⁶⁾ pointed out the possibility of the GaAs crystal growth from Ga droplets by a vapor-liquid-solid (VLS) mechanism. Since the surface of the droplets is thought to be an effectively random high-index or roughened surface with many available sites for the adsorption of the As atom at the liquid-vapor interface, the sticking coefficient of the As atoms to the Ga droplets is nearly 1 as reported by Hirth and Pound.¹⁷⁾

In contrast, two-dimensional lateral growth of GaAs occurred on the As-adsorbed $c(4 \times 4)$ surface. Figure 5 shows the RHEED intensity variations during Ga deposition and subsequent As molecular beam irradiation on the $c(4 \times 4)$ surface at 200°C . In this case, the specular beam intensity decreased first and then increased to a maximum value during Ga deposition and decreased again with appearance of the halo. The specular beam intensity reached a maximum value after the Ga deposition corresponding to an amount required to form one monolayer of GaAs and the appearance of the halo during Ga deposition corresponded to the amount required to form about 1.7 equivalent monolayer of GaAs, which is the same phenomenon observed by Horikoshi and

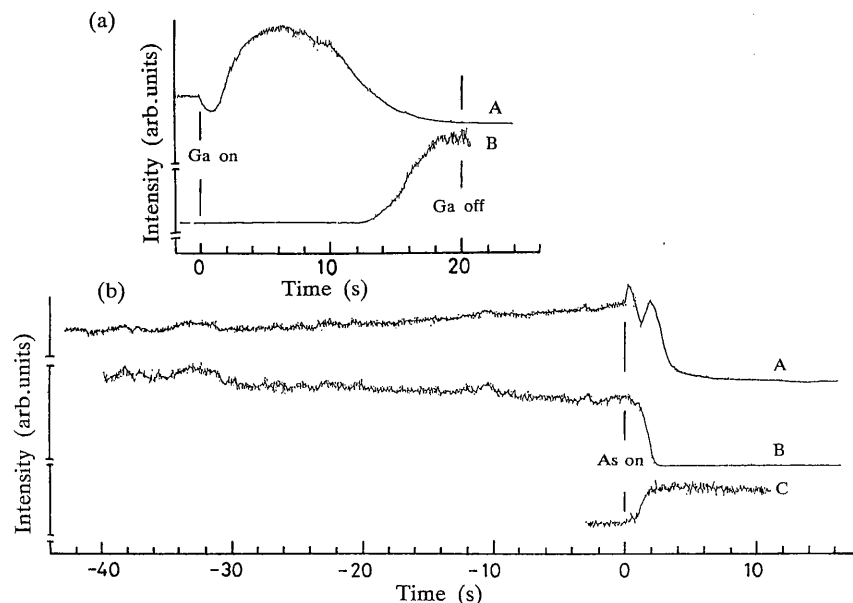


Fig. 5. The variations in the RHEED intensities during Ga deposition (a) and the As molecular beam irradiation (b) on the As-adsorbed GaAs substrate at 200°C. A, B and C correspond to the specular beam, halo and (004) transmission spot intensities, respectively.

Kawashima¹⁸⁾ for the low-temperature growth of GaAs thin films by alternating supplies of Ga and As to the As-adsorbed GaAs substrate. Similar results were obtained by Deparis and Massies¹⁹⁾ for the Ga deposition on the GaAs (001) surface with $c(4 \times 4)$ reconstruction. Although Horikoshi and Kawashima and Deparis and Massies have not observed the halo intensity change, the fact that the halo appeared after the deposition of 1.7 equivalent monolayers of Ga indicates that the surface coverage of As atoms is 1.7 for $c(4 \times 4)$ reconstruction, which is nearly equal to the value obtained by Biegelsen *et al.*²⁰⁾

The specular beam intensity increased first by the As molecular beam irradiation to the surface, then decreased, increased again and finally decreased. The intensity change in the specular beam is very similar to the MEE growth at low substrate temperatures. Deparis and Massies observed the RHEED pattern change during As molecular beam irradiation to the Ga-stabilized surface. In their results, the As-stabilized (2×4) surface reconstruction appeared at the first and second maxima and the Ga-stabilized (4×2) surface reconstruction appeared at the minimum of the specular beam intensity change during As molecular beam irradiation. This is due to the difference in the specular beam intensities between the As- and Ga-stabilized surfaces. In our work, we could not identify the change in the RHEED pattern, because a diffused pattern appeared during As molecular beam irradiation. However, the (1×3) surface reconstruction, which was caused by an As-adsorption phase¹⁴⁾ below 300°C, appeared in the final stage instead of $c(4 \times 4)$ reconstruction in Deparis and Massies' results. These differences between our results and Deparis and Massies' results are ascribed to the differences in the substrate temperature during As molecular beam irradiation. They main-

tained the substrate temperature at about 400°C, but we kept the substrate temperature at 200°C. Well-defined surface structure is not expected to appear at a low substrate temperature.

The halo intensity decreased rapidly at the minimum specular beam intensity. This indicates that layer-by-layer growth was predominant. However, three-dimensional growth also occurred because the (004) transmission intensity increased, in this case, due to As molecular beam irradiation to the Ga droplets deposited on the substrate as in the case of the ordinary MEE process.²¹⁾ The specular beam intensity increased and the halo intensity decreased slightly before the opening of the As cell shutter. This is caused by initiation of the GaAs crystal growth at the As background pressure of about 5×10^{-8} Torr.

3.3 Surface morphology

The surface morphologies of the samples after Ga deposition and subsequent As molecular beam irradiation observed by HRSEM are shown in Fig. 6 for the S-terminated GaAs substrate. Many hemispherical Ga droplets were formed on the S-terminated surface after the Ga deposition. The average diameter of the Ga droplets is 240 Å and the standard deviation of the size distribution is about 15%. The total amount of Ga in the droplets estimated from the hemispherical shape and the diameter is 2.7 equivalent GaAs layers, which corresponds to the total number of supplied Ga atoms. This indicates that the Ga atoms coalesced without reaction with the surface as speculated from the RHEED pattern changes discussed above. These Ga droplets became microcrystals with rectangular bases and (111) facets after the As molecular beam irradiation. The base dimensions of the microcrystals are 250 Å \times 430 Å with standard deviation of each dimension of

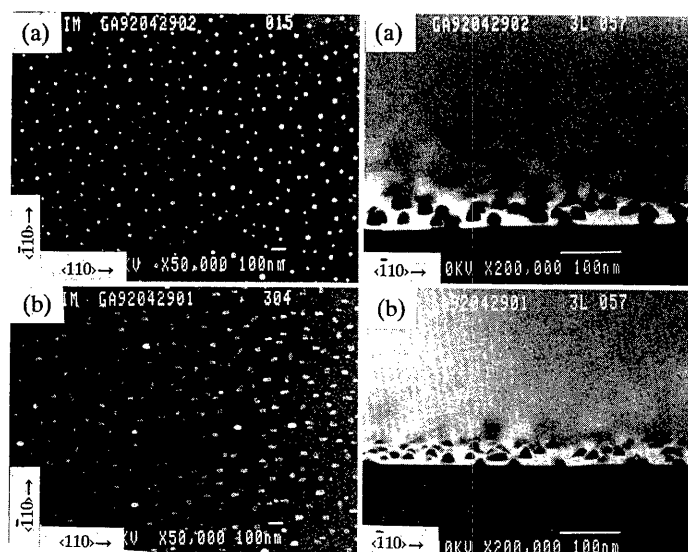


Fig. 6. Surface morphologies of the samples after Ga deposition (a) and subsequent As molecular beam irradiation (b) on S-terminated GaAs (001) at 200°C. Left column: top views; right column: side views.

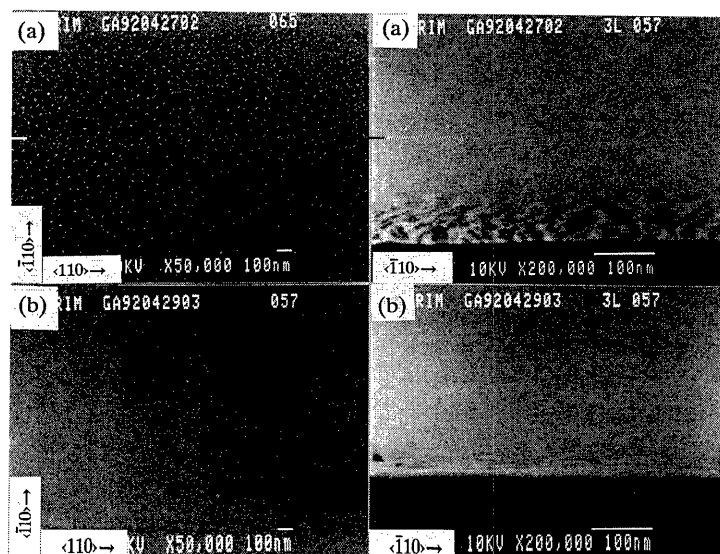


Fig. 7. Surface morphologies of the samples after Ga deposition (a) and subsequent As molecular beam irradiation (b) on As-adsorbed GaAs (001) at 200°C. Left column: top views; right column: side views.

about 20%. The length of the shorter edge of the microcrystals is nearly equal to the diameter of the Ga droplets. Most microcrystals were enlarged in the $\langle 110 \rangle$ direction as in the case of InSb microcrystals grown on a CdTe substrate by droplet epitaxy. The height of the microcrystal is about 150 Å. The (111) facets are not well defined compared with the $(\bar{1}\bar{1}1)$ facets. However, the total amount of Ga in the microcrystals is estimated as about 2.7 equivalent GaAs layers if we assume that the microcrystals are surrounded by complete (111) facets.

Figure 7 shows the surface morphologies after the Ga deposition and subsequent As molecular beam irradiation on the $c(4 \times 4)$ As-adsorbed GaAs surface. Ga droplets appeared on the surface; however, the average diameter of the Ga droplets is smaller and the densities

are higher than those of Ga droplets deposited on the S-terminated surface. Although the shape of the Ga



Fig. 8. Slightly oblique side view of the Ga droplet deposited on S-terminated GaAs (001) at 350°C.

droplets is not clear in Fig. 7, the contact angle is estimated as about 70° from the side-view observation of the Ga droplets deposited on the As-adsorbed GaAs substrate at 450°C since we can obtain larger droplets (about 1500 \AA diameter) at this substrate temperature. The total amount of Ga in the droplets is estimated as about 1 equivalent GaAs layer using this contact angle and the observed diameter of the droplets. The remaining deposited Ga atoms disappeared with the formation of the Ga-stabilized GaAs surface in this case. A smooth surface was obtained by the subsequent As molecular beam irradiation to the Ga deposited surface on the As-adsorbed GaAs surface.

These results revealed that three-dimensional growth of GaAs epitaxial microcrystals occurred on the S-terminated GaAs surface, whereas two-dimensional growth of GaAs occurred predominantly on the As-adsorbed surface by the successive irradiation of Ga and As molecular beams to the substrate. The three-dimensional growth of GaAs microcrystals is caused by the inertness for the adsorption of Ga and As atoms. The epitaxial growth of GaAs microcrystals originates from the nearly equal lattice constants of the S-terminated GaAs surface and the microcrystals.

The surface morphology of the S-terminated surface with Ga droplets deposited at 350°C is shown in Fig. 8.

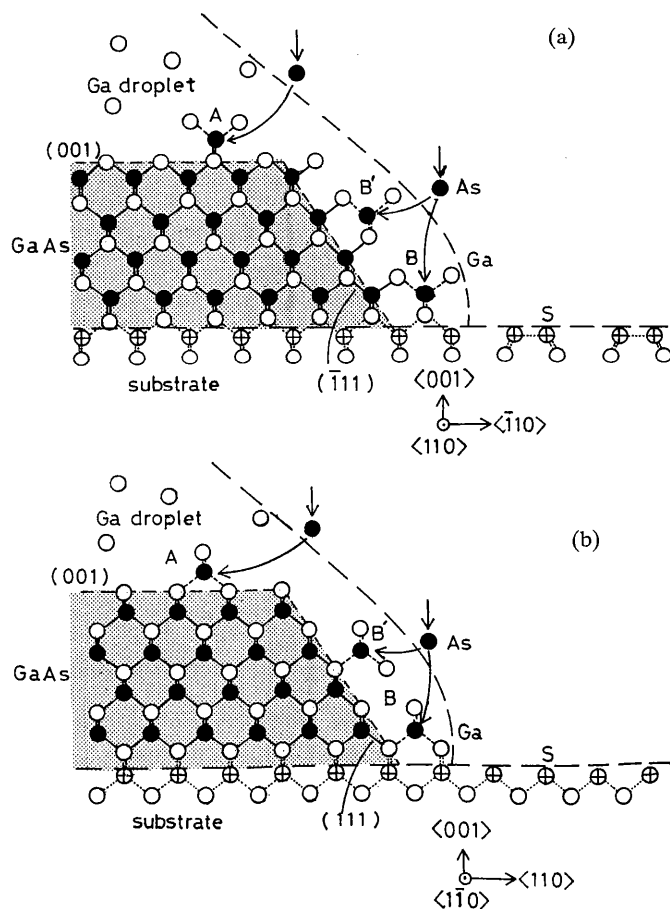


Fig. 9. Schematic explanation of growth mechanism of the GaAs microcrystals on S-terminated GaAs (001): (a) cross-sectional view along the $\langle 110 \rangle$ azimuth; (b) cross-sectional view along the $\langle 1\bar{1}0 \rangle$ azimuth.

The contact angles of some Ga droplets are less than 90° . However, the angle is nearly 90° in the case of Ga droplets deposited on the S-terminated substrate at 200°C . This probably originates from the reaction between the deposited Ga and S on the GaAs surface at 350°C as speculated above.

Figure 9 shows the speculated growth mechanism of the GaAs epitaxial microcrystals. Dissolved As atoms in the Ga droplets diffuse into the interface of Ga- and S-terminated GaAs. Then GaAs is crystallized at the interface epitaxially. The microcrystals of GaAs grow with the adsorption of As atoms such as A and B in the figure. It is important to note that the growth of GaAs microcrystals occurred in the Ga droplets. Then the incorporated As atoms combined with four Ga atoms on each surface as shown in the figure. On the $(\bar{1}11)$ surface, B and B' are nearly equivalent sites; however, site B is more stable than site B' on the (111) surface. Thus, the well-defined $(\bar{1}11)$ facet appears but the (111) facet is not as clear. Also, increase in the base size of the microcrystal occurs more easily in the $\langle 110 \rangle$ direction than in the $\langle \bar{1}10 \rangle$ direction, because the As atom at site B' on the (111) surface readily redissolves and settles at the more stable B-like site adjacent to B.

The anisotropy of the GaAs microcrystal base size is also explained by the surface structure of S-terminated GaAs. The (2×1) surface structure of S-terminated GaAs is believed to be caused by the S-S dimer rows. Generation of an unstable nondimerized S row or rearrangement of an S dimer is necessary to expand the base size in the $\langle \bar{1}10 \rangle$ direction by adsorption of Ga atoms from Ga droplets. However, only destruction of S dimer rows is sufficient for the expansion of the base size in the $\langle 110 \rangle$ direction.

Although only a monolayer of S atoms is thought to exist on the surface of S-terminated GaAs, the formation of a thin Ga_2Se_3 -related compounds layer near the surface is suggested by the photoemission spectroscopy study of the Se-terminated GaAs surface.^{22,23)} The interface structure between GaAs microcrystals and the substrate is not clear at this point. It is necessary to investigate further the interface structure between GaAs microcrystals and the S-terminated GaAs substrate.

4. Conclusions

We have investigated Ga droplets and GaAs microcrystal formation during Ga deposition and subsequent As molecular beam irradiation on the S-terminated substrate. Numerous hemispherical Ga droplets with a diameter of 240 \AA were formed on the substrate at 200°C . The Ga droplets became GaAs epitaxial microcrystals with rectangular bases and (111) facets with this procedure. The average base size of the GaAs microcrystals was about $250 \text{ \AA} \times 430 \text{ \AA}$, and the height was about 150 \AA . The growth mechanism is thought to be of a vapor-liquid-solid (VLS) mechanism. We can use this method to fabricate GaAs quantum well boxes using the S-, Se- or Te-terminated GaAlAs epitaxial layer and the subsequent overgrowth of the GaAlAs layer covering the GaAs microcrystals.

Acknowledgments

The authors wish to acknowledge many valuable discussions with Drs. T. Chikyow and H. Noerenberg of the National Research Institute for Metals. Appreciation is also expressed to S. Takahashi of the same institute for HRSEM observations.

- 1) H. Sakaki: Jpn. J. Appl. Phys. **28** (1989) L314.
- 2) Y. Arakawa and H. Sakaki: Appl. Phys. Lett. **40** (1982) 939.
- 3) T. Fukui, S. Ando, Y. Tokura and T. Toriyama: Appl. Phys. Lett. **58** (1991) 2018.
- 4) N. Koguchi, S. Takahashi and T. Chikyow: J. Cryst. Growth **111** (1991) 688.
- 5) S. Takahashi and N. Koguchi: 9th Symp. Record of Alloy Semiconductor Physics and Electronics, 1990, p. 117.
- 6) T. Chikyow and N. Koguchi: Jpn. J. Appl. Phys. **29** (1990) L2093.
- 7) Y. Nannichi, J. F. Fan, H. Oigawa and A. Koma: Jpn. J. Appl. Phys. **27** (1988) L2367.
- 8) T. Ohno and K. Shiraishi: Phys. Rev. B **42** (1990) 11194.
- 9) H. Oigawa, J. F. Fan, Y. Nannichi, H. Sugahara and M. Oshima: Jpn. J. Appl. Phys. **30** (1991) L322.
- 10) T. Ohno: Surf. Sci. **255** (1991) 299.
- 11) T. A. Flaim and P. E. Ownby: J. Vac. Sci. & Technol. **8** (1971) 661.
- 12) C. E. C. Wood, D. DeSimone, K. Singer and G. W. Wicks: J. Appl. Phys. **53** (1982) 4230.
- 13) Y. Horikoshi, M. Kawashima and H. Yamaguchi: Jpn. J. Appl. Phys. **27** (1988) 169.
- 14) L. Daweritz and R. Hey: Surf. Sci. **236** (1990) 15.
- 15) O. Kubaschewski and C. B. Alcock: *Metallurgical Thermochemistry* (Pergamon Press, Oxford, 1979) 5th ed.
- 16) R. S. Wagner and W. C. Ellis: Appl. Phys. Lett. **4** (1964) 89.
- 17) J. P. Hirth and G. M. Pound: J. Phys. Chem. **64** (1960) 619.
- 18) Y. Horikoshi and M. Kawashima: Jpn. J. Appl. Phys. **28** (1989) 200.
- 19) C. Deparis and J. Massies: J. Crystal Growth **108** (1991) 157.
- 20) D. K. Biegelsen, R. D. Bringans, J. E. Northrup and L. E. Swartz: Phys. Rev. B **41** (1990) 5701.
- 21) J. Osaka, N. Inoue, Y. Mada, K. Yamada and K. Wada: J. Cryst. Growth **99** (1990) 120.
- 22) S. Takatani, A. Nakano, K. Ogata and T. Kikawa: Jpn. J. Appl. Phys. **31** (1992) L458.
- 23) S. Takatani, T. Kikawa and M. Nakazawa: Phys. Rev. B **45** (1992) 8498.